The EMBO Journal vol.15 no.21 pp.5907–5916, 1996

Transcription antitermination regulation of the *Pseudomonas aeruginosa* amidase operon

Stuart A.Wilson[1], Simon J.M.Wachira[2], Richard A.Norman, Laurence H.Pearl and Robert E.Drew[3]

Department of Biochemistry, University College London, Gower Street, London WC1E 6BT, UK

[1]Present address: Department of Biochemistry, University of Oxford, South Parks Road, Oxford, OX1 3QU, UK
[2]Present address: Department of Biochemistry, University of Nairobi, PO Box 30197, Nairobi, Kenya

[3]Corresponding author

***In vivo* titration experiments have demonstrated a direct interaction between the *Pseudomonas aeruginosa* transcription antiterminator, AmiR, and the mRNA leader sequence of the amidase operon. A region of 39 nucleotides has been identified which is sufficient to partially titrate out the AmiR available for antitermination. Site-directed mutagenesis has shown that the leader open reading frame has no role in the antitermination reaction, and has identified two critical elements at the 5′ and 3′ ends of the proposed AmiR binding site which are independently essential for antitermination. A T7 promoter/RNA polymerase-driven system shows AmiR-mediated antitermination, demonstrating a lack of promoter/polymerase specificity. Using the operon negative regulator, AmiC, immobilized on a solid support and gel filtration chromatography, an AmiC–AmiR complex has been identified and isolated. Complex stability and molecular weight assayed by gel filtration alter depending on the type of amide bound to AmiC. AmiC–AmiR-anti-inducer is a stable dimer–dimer complex and the addition of the inducer, acetamide, causes a conformational change which alters the complex stability and either this new configuration or dissociated AmiR interacts with the leader mRNA to cause antitermination.**

Keywords: amidase/antitermination/*P.aeruginosa*

Introduction

Pseudomonas aeruginosa is able to grow on short chain-length aliphatic amides by virtue of a chromosomally encoded aliphatic amidase (EC 3.5.1.4) (Kelly and Clarke, 1962). Amidase activity is inducible by the 2- and 3-carbon amides, acetamide and propionamide, but butyramide (4C) acts as an anti-inducer (Brammar and Clarke, 1964). Two regulatory genes which lie ≈2 kilobases downstream of the amidase structural gene (*amiE*) have been identified and sequenced (Figure 1A) (Cousens *et al.*, 1987; Lowe *et al.*, 1989; Wilson and Drew, 1991). *amiR* encodes a transcription antitermination factor which, under inducing conditions, mediates the extension of a short, constitutively produced, leader transcript through a rho-independent transcription terminator and into the amidase operon (Drew and Lowe, 1989; Wilson and Drew, 1995). The second regulatory protein, AmiC, negatively regulates amidase expression and disruption of the *amiC* open reading frame (ORF) leads to constitutive amidase expression (Wilson and Drew, 1991). Complementation studies have shown that AmiR functions independently of inducing/anti-inducing amides (Cousens *et al.*, 1987; Wilson and Drew, 1991). However, a fully inducible amidase system can be reconstituted in *Escherichia coli* with the *amiE*, *amiC* and *amiR* genes alone. AmiC thus confers inducibility and amide sensitivity on the system and binds both inducing and non-inducing amides (Wilson *et al.*, 1993). *In vivo* experiments suggest that the mechanism of AmiC inhibition of amidase expression involves a direct protein–protein interaction with AmiR and that to preserve inducibility, stoichiometric amounts of AmiC and AmiR must be maintained (Wilson and Drew, 1991; Wilson *et al.*, 1993).

The DNA sequence upstream of the *amiE* gene contains an *E.coli*-like promoter sequence (pE), a short ORF of unknown function, a rho-independent transcription termination sequence (T1) and then the *amiE* Shine–Dalgarno sequence and gene (Figure 1B and C). The proposal of the antitermination model initially came from the analysis of a terminator deletion construct which led to amide-independent, AmiR-independent, constitutive amidase expression (Drew and Lowe, 1989). The model has been substantiated by mapping the transcription start-point to the promoter region and showing constitutive production of the leader mRNA (Wilson and Drew, 1995). Northern blot analysis and S1 mapping have shown that transcripts reading through T1 can continue through the entire operon. Thus, AmiC and AmiR form an autogenous control circuit, regulating their own expression and amidase expression in response to inducing amides (Wilson and Drew, 1995).

Several different types of prokaryotic system have been identified as subject to regulation by transcription antitermination mechanisms. These include *rrn* operon expression in *E.coli* (Squires *et al.*, 1993), lambdoid bacteriophage delayed early and late gene expression (Roberts, 1988), and the *bgl* and *sac* catabolic systems in *E.coli* and *Bacillus subtilis* respectively (Mahadevan and Wright, 1987; Le Coq *et al.*, 1989). From an overall structural/functional point of view the two inducible catabolic operons appear to be most similar to the amidase system. In both *bgl* and *sac*, inducible gene expression is exerted via a negative control inducer-binding sensor protein and an antitermination factor regulator. The relevant antiterminators SacY, SacT and BglG are homologous (Amster-Choder and Wright, 1993) and seem to form a family distinct from the non-homologous AmiR.

© Oxford University Press

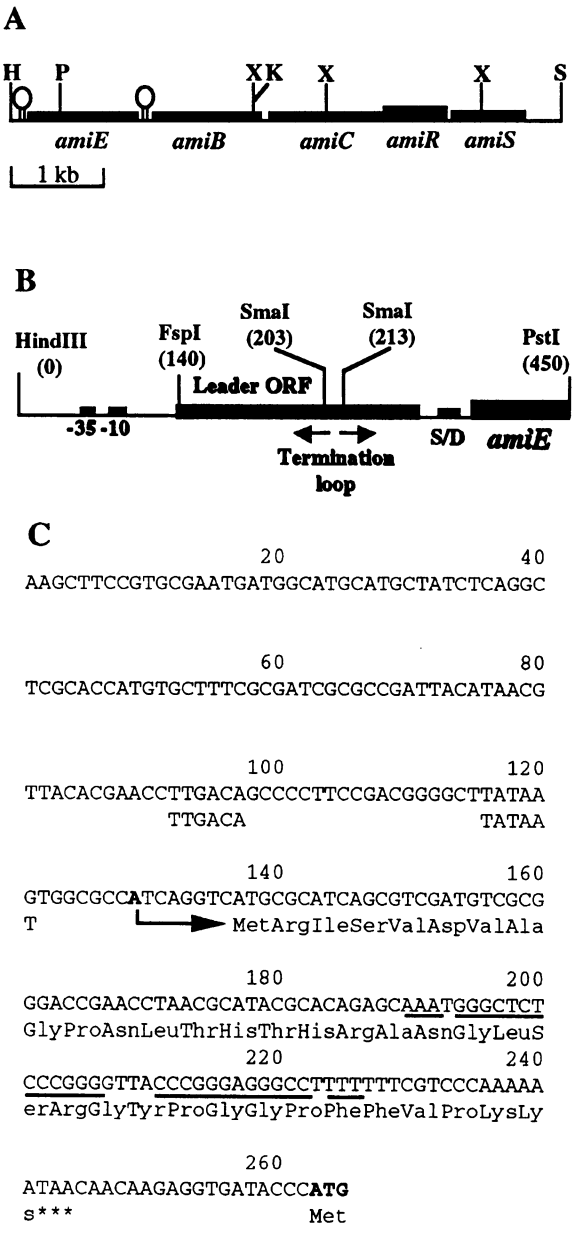

Fig. 1. Amidase operon of *P.aeruginosa*. (**A**) Gene organization of amidase operon. Restriction sites are H (*Hin*dIII), P (*Pst*I), X (*Xho*I), K (*Kpn*I) and S (*Sal*I). (**B**) Amidase operon leader region. Locations of the σ70 promoter sequences, the leader open reading frame (ORF), the rho-independent transcription terminator, the *amiE* gene Shine–Dalgarno sequence (S/D), the start of the *amiE* gene and some of the restriction enzyme target sites are shown. (**C**) DNA sequence of the amidase operon leader region. The sequence of the plus strand runs from the *Hin*dIII site to the start of the *amiE* gene. The sequence of the *E.coli* consensus promoter is shown below, 92–97 (–35) and 116–121 (–10). The transcription start point (129) is shown in bold. The leader ORF is translated, the transcription terminator is shown by underlining and the *amiE* start codon is in bold.

When activated, these proteins prevent transcription termination at sites within operon leader regions by binding to related, imperfectly palindromic, 29-base RNA (RAT) sequences located upstream and partially overlapping the termination loops. These systems are sufficiently related such that RAT sequence-directed mutagenesis can change the antitermination factor specificity of the interaction (Aymerich and Steinmetz, 1992).

In this paper we report the results of *in vivo* and *in vitro* studies to investigate the mechanism of the AmiR-mediated *P.aeruginosa* amidase, antitermination reaction at the T1 terminator, and *in vitro* investigations of the AmiC–AmiR interaction.

Results

In vivo studies of the transcription antitermination reaction

The sequence homology between the amidase operon leader region and the RNA binding site for the BglG transcription antiterminator (Drew and Lowe, 1989) suggested that, mechanistically, the systems might be similar. Thus, to test the proposal that AmiR bound directly to the leader mRNA, a two-plasmid system was developed in which high levels of amidase were synthesized by provision of AmiR *in trans*, and a third plasmid capable of expressing just the leader mRNA was added to titrate out the AmiR. *E.coli* JA221,pTM1(*amiE*) produces a background level of amidase-specific activity (SA) of 0.7. JA221,pTM1,pSW35(*amiR*), in which *amiR* is expressed from a vector promoter, generates a constitutive amidase SA of 41.5. To this system was added a third compatible plasmid (pSW66), a pGEM3Z derivative carrying the leader region *Fsp*I–*Pst*I fragment (Figure 1B) which can only be expressed from the vector T7 promoter. The SA from this strain (JA221, pTM1, pSW35, pSW66) of 37.5 shows a slight reduction of AmiR-dependent amidase activity when the competing leader sequence is not expressed. Expression was measured in strain DE3 in which T7 polymerase is produced. With DE3, pTM1, pSW35, pGEM3Z as a control, a SA of 37.0 is observed, showing that the system is functionally comparable with JA221. In DE3, pTM1, pSW35, pSW66 the SA is reduced to 22.3, showing specific titration of the AmiR by the T7-expressed leader RNA from pSW66. A similar titration is seen using pMW42 (SA 22.8) which is a pGEM4Z derivative carrying the leader *Hin*dIII–*Pst*I region expressed from the vector T7 promoter in place of pSW66. The *in vivo* titration causes an ~40% decrease in amidase activity, and the comparison between expression in JA221 and DE3 shows that the effect is not a DNA titration but only occurs if the leader mRNA is expressed. To define the competing sequences more thoroughly, plasmid pSW76 was constructed. This contains residues 164–203 (Figure 1C) cloned into pGEM3Z where the shortened leader sequence may only be expressed from the vector T7 promoter. Expression from DE3, pTM1, pSW35, pSW76 gave a SA of 24.1, clearly showing titration of AmiR with a short, 39-residue leader RNA sequence.

As a measure of the amount and stability of leader transcript produced in the *in vivo* titration experiments, Northern slot blot analysis was performed on total cellular RNA probed with the *Hin*dIII–*Pst*I DNA fragment (see Table Va). DE3,pTM1 showed 44.1 units and the addition of *amiR* (DE3,pTM1,pSW35) increased the hybridization to 103.3 units due to either increased stability or recovery of the longer antiterminated transcripts. Somewhat surprisingly, the value for DE3,pSW66 in which the competing leader was synthesized from the vector T7 promoter was only 14.8 units. This explains the inability in these studies to completely compete out AmiR. Thus, these results

clearly implicate AmiR in a direct interaction with the leader mRNA sequence and start to define regions important in the interaction. The context in which the leader RNA is expressed appears to be unimportant for titration since all of these constructs produce *ami* leader–pGEM hybrid transcripts.

Promoter and polymerase independence of the transcription antitermination reaction

To investigate RNA polymerase/promoter dependence of the antitermination reaction, plasmid pSW69 was constructed. This pGEM3Z derivative contains the *Fsp*I to *Xho*I fragment, carrying the *amiE* leader region and gene, but deleted for pE, in an orientation such that expression of *amiE* can only occur from the vector T7 promoter. Amidase activity was measured initially in *E.coli* JA221,pSW69 and JA221, pSW69, pSW35(*amiR*). No amidase activity was present within either isolate as the strain lacks the T7 RNA polymerase. Activity was then measured in *E.coli* DE3, pSW69 and DE3, pSW69, pSW35. Regulation of T7 RNA polymerase expression in DE3 is leaky and assays were performed in the absence of the inducer IPTG. Assays in DE3, pSW69 showed a SA of 24.6 and in DE3, pSW69, pSW35 a SA of 47.9. These results show firstly that T7 polymerase is able to partially read through the leader region terminator (T1) and secondly with this system that the presence of AmiR leads to antitermination and increased amidase expression. The T7 expression studies confirm *in vitro* investigations in which the production of T7 run-off transcripts is seen to be ~50% terminated by the T1 terminator (unpublished data).

These experiments show that, in the amidase antitermination regulatory system, the reaction is neither promoter- nor RNA polymerase-specific. These results thus strongly indicate that the mechanism of antitermination is most likely to be RNA leader sequence-dependent and similar to the *bgl* and *sac* systems (Aymerich and Steinmetz, 1992).

In vitro mutagenesis of the mRNA leader region.

The amidase operon upstream region produces, under non-inducing conditions, a short leader mRNA containing a 35-amino acid ORF (Figure 1C) (Wilson and Drew, 1995). The leader RNA can be folded into a stable structure (–43.7 kcal/mol) containing two large stem–loops (Figure 2), which presumably reflects the *in vivo* situation. Residues 5–37 form a hairpin loop with a free energy of formation of –16.1 kcal/mol; there is then a central region containing little secondary structure (residues 38–65), although a minor loop (53–61) is possible, and finally the rho-independent termination loop (residues 66–95) with a free energy of formation of –23.3 kcal/mol (Drew and Lowe, 1989).

Investigation of the leader ORF

The *in vivo* titration studies strongly indicated that antitermination occurred by direct interaction of AmiR with the mRNA leader region. The subsequent use of the T7 expression system showed that the antitermination reaction was dependent on (i) AmiR, and (ii) the leader region mRNA, but was not promoter/polymerase-specific. To investigate the phenomenon further, we initially looked at the role of the leader region ORF in the reaction. Plasmid

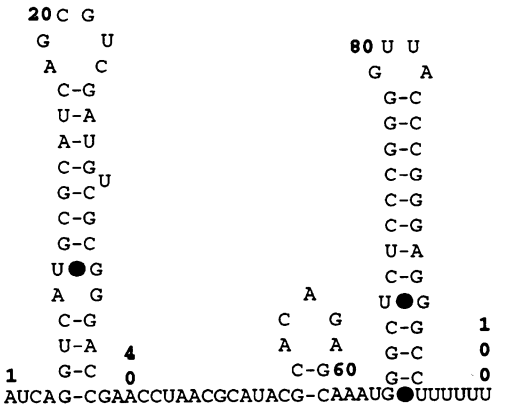

Fig. 2. RNA fold of the leader region transcript residues 1–100. Complementary residues are shown by lines and G–U interactions by filled circles (Zuker, 1989; Jaeger *et al.*, 1989a,b).

pMW11 has a stop codon inserted into the ORF at amino acid 9 (G→T, 161[33]) and pSB102 has a T inserted at position 164[36], which creates a novel *Bam*I target and causes extension of the leader ORF such that it continues into the *amiE* gene out of frame. Amidase activity was measured in *E.coli* JA221 containing plasmids pSB101 (the wild-type), pMW11 and pSB102 by themselves and also with pSW35, a compatible *amiR* expression vector. The sequence changes and results of the assays are shown in Table Ia. In this assay system, in the absence of the *amiR* gene, any amidase activity must occur by readthrough of the T1 terminator, and activity in the presence of *amiR* is a measure of the antitermination activity of AmiR and reflects AmiR binding to the leader region. pSB101 (WT) shows low amidase specific activity (1.2) and, in the presence of pSW35, a high antiterminated specific activity of 42.0. The insertion of the stop codon into pMW11 increases amidase-specific activity in both the absence and presence of AmiR (4.6; 65.3). With pSB102, specific activities of 3.2 and 49.1 are found in the absence and presence of *amiR*. It is evident that these changes to the leader ORF have no detrimental effects on the antitermination reaction. This clearly demonstrates that the ORF is not involved in antitermination and indicates, from the result with pSB102, that the ORF is probably not translated.

Identification of the AmiR interaction region

The central non-structured section of the leader region is that identified previously as showing quasi-homology to the *bgl* RAT sequence (Drew and Lowe, 1989). This region of 30 residues is unusual for *P.aeruginosa* (GC ratio of 65%) in that it contains 12 As, 10 Cs, five Gs and three U residues. We have now made changes in this region to investigate the antitermination reaction. For ease of recombinant identification, DNA sequences were initially changed by *in vitro* mutagenesis to place *Bam*I restriction enzyme target sites at a variety of locations between positions 36 (164) and 62 (190), the start of the termination loop. This strategy meant that rarely were the mutations single changes, making the interpretation of the results more complex. However, it offered the opportunity for *in vitro* recombination between the *Bam*I targets situated at different positions, to create insertions and deletions, and the possibility of restriction enzyme cleavage and trimming, or cleavage, partial filling and trimming

Table I. Measurement of antitermination in constructs with changes upstream of position 36

		Fold energy		
		–AmiR	+AmiR	1–45
a				
pSB101	GAU GUC GCG GGA CCG AAC CUA	1.2	42.0	–16.1
pMW11	GAU GUC GCG uGA CCG AAC CUA	4.6	65.3	–20.0
pSB102	G AUG UCG CGG GAu CCG AAC CUA	3.2	49.1	–13.5
b				
pMW13	GU AGU CGC GGG Acg gau CCG AAC CUA	0.3	33.6	–13.5
pSW61	G AUG UCG CGG GAc gau CCG AAC CUA	4.2	28.4	–13.0
	*			
	AUC AGC GUC GAU GUC GCG GGA CCG AAC CUA ACG CAU ACG CAC AGA GCA AAU			

(**a**) Measurement of changes to the leader ORF. pSB101 is the wild-type, pMW11 has a stop codon at aa 9, and in pSB102 the T insert at position 36 extends the ORF. Residues 36–41 are underlined.
(**b**) Other upstream changes. pMW13 contains a 5 bp insertion and pSW61 a 4 bp insertion.
The wild-type transcript residues 15 to 65 is shown underneath. Position 36 is marked * and the start of the termination stem/loop is shown by underlining.
Amidase activities were measured in *E.coli* JA221 with these constructs (–AmiR) and in the presence of an *amiR* expression vector, pSW35 (+AmiR).
The leader sequences 1–45 (in pSB101) or the equivalent position were subject to MFold and the calculated free energy of loop formation (kcal/mol) is shown as Fold energy (Zucker, 1989; Jaeger *et al.*, 1989a,b).

Table II. Measurement of antitermination in constructs with changes to the L (36–41) region

		Fold energy		
		–AmiR	+AmiR	1–45
pSB101	GAU GUC GCG GGA CCG AAC CUA	1.2	42.0	–16.1
pSB103	GAU GUC GCG GGA CgG AuC CUA	1.1	26.0	–13.5
pSW60	GAU GUC GCG GGA uCG AuC CUA	0	2.4	–13.1
pSW64	GAU GUC GCG gCG AAC CUA	1.3	34.0	–12.3
pMW12	GA UGU CGC ggG AuC CUA	0.1	3.2	–13.0
	*			
	AUC AGC GUC GAU GUC GCG GGA CCG AAC CUA ACG CAU ACG CAC AGA GCA AAU			

pSB101 is the wild-type, pSB103 and pSW60 have two base substitutions, pSW64 has a three base deletion and pMW12 has a four base deletion. Residues 36–41 are underlined.
The wild-type transcript residues 15 to 65 is shown underneath. Position 36 is marked * and the start of the termination stem/loop is shown by underlining.
Activities were measured as described in Table I.
The leader sequences 1–45 (in pSB101) or the equivalent position were subject to MFold and the calculated free energy of loop formation (kcal/mol) is shown as Fold energy (Zucker, 1989; Jaeger *et al.*, 1989a,b).

to further investigate the sequences. To investigate the role of the sequences of the termination loop itself in the antitermination reaction, the *Sma*I targets present in both the up and down side of the stem–loop (Figure 1C) were changed to *Sst*II (CCCGGG to CC**G**CGG) targets (pMW10). With these changes the loop stability is not affected. JA221, pMW10 showed specific activities (2.9 for –AmiR; 67.6 for +AmiR) comparable with wild-type levels. Therefore, these upper stem sequences do not appear to be involved in the antitermination reaction.

Five parental plasmids were initially constructed with *Bam*I targets at different positions along the 30-nucleotide sequence thought to interact with AmiR. Derivative constructs were then made which have further changes. The results are grouped together showing changes at four locations: upstream of the left (L:36) region, and within the L (36–41), middle (M: 42–53) and right (R: 54–62) regions. Amidase activities were measured for the wild-type (pSB101) and mutant plasmids with and without AmiR.

Amidase activities from plasmids with sequence changes upstream of position 36 are shown in Table I (a and b). pSB101, pMW11 and pSB102 have been described above. pMW13 carries a 5 bp insertion and pSW61 a 4 bp insertion compared with the WT (pSB101). The sequences have been lined up with respect to the termination loop (on the right). Each of these mutants shows high AmiR-dependent antitermination activity similar to the WT, except for pMW13 and pSW61, where activities are somewhat reduced. Additionally, with these examples secondary structure folds (not shown) of residues 1 to the CCTAA (residue 45 in pSB101) offers some evidence to support a proposal that decreased stability of Loop 1 leads to a reduction in the AmiR-dependent antitermination reaction.

Multiple changes to the 36–41 (L) region can lead to an almost complete inactivation of antitermination (Table II). The sequences shown in Table II have again been aligned to the right and show the amidase-specific activities in the absence and presence of AmiR and the calculated free energy of formation of Loop 1. Not all

Table III. Measurement of antitermination in constructs with changes to the M (42–53) region

		Fold energy		
		–AmiR	+AmiR	38—TT
a				
pSB101	CCG AAC CUA ACG CAU ACG CAC AGA GCA AAU	1.2	42.0	–8.2
pMW25	CCG AAC Cgg Auc CAU ACG CAC AGA GCA AAU	0.4	37.2	–9.9
pMW26	CCG AAC CUA ACG gAU cCG CAC AGA GCA AAU	0.3	19.9	–9.0
pSW73	CC GAA CCG gAU cCG CAC AGA GCA AAU	4.5	16.7	–8.7
pSW70	CC GAA CCG CAU ACG CAC AGA GCA AAU	10.3	39.2	–8.2
pSW62	C CGA ACC ggA ucg Auc CAU ACG CAC AGA GCA AAU	8.9	20.8	–11.3
pSW63	C CGA ACC UAA Cgg Auc gAU cCG CAC AGA GCA AAU	3.0	18.1	–9.7
pSW71	C CGA ACC UAA Cgg Auc CAU ACG CAC AGA GCA AAU	14.1	19.3	–10.9
b				
pSB101	GGA CCG AAC CUA ACG CAU ACG CAC AGA GCA AAU	1.2	42.0	
pSB103	GGA CgG AuC CUA ACG CAU ACG CAC AGA GCA AAU	1.1	26.0	
pSW74	GGA CgG A.. ... .uc CAU ACG CAC AGA GCA AAU	2.9	15.4	
pSW75	GGA CgG A.. ... ..U cCG CAC AGA GCA AAU	1.6	9.8	
	GCG GGA CCG AAC CUA ACG CAU ACG CAC AGA GCA AAU			

(**a**) pSB101 is the wild-type, pMW25 has a four base substitution, pMW26 has a two base substitution, pSW73 and pSW70 have four base deletions and pSW62, 63 and 71 have four base insertions. L (36–41) and R (54–62) regions are underlined. Activities are presented as described in Table I. The leader sequences 38 to GGGT in the transcription terminator were subject to MFold and the calculated free energy of loop formation (kcal/mol) is shown as Fold energy (Zucker, 1989; Jaeger *et al.*, 1989a,b).
(**b**) pSB101 is the wild-type and pSB103 has two substitutions in the L region. pSW74 and pSW75 have the same mutant L region as pSB103 but also contain respectively six and ten base deletions bringing the L and R regions closer together.
The wild-type transcript residues 30–65 is shown underneath in which the start of the termination stem–loop is shown by underlining.

Table IV. Measurement of antitermination in constructs with changes to the R (54–62) region

		–AmiR	+AmiR
pSB101	CCG AAC CUA ACG CAU ACG CAC AGA GCA AAU	1.2	42.0
pMW27	CG AAC CUA ACG CAU ACG gAu ccA GCA AAU	0.1	1.5
pMW28	CCG AAC CUA ACG CAU ACG CAC gGA uCc AAU	0.1	0.9
pSW72	CCG AAC CUA ACG CAU ACG CAC gGauccA GCA AAU	0	4.2
	GCG GGA CCG AAC CUA ACG CAU ACG CAC AGA GCA AAU		

pSB101 is the wild-type, pMW27 has a four base substitution, pMW28 has a three base substitution, pSW72 has a three base insertion. L (36–41) and R (54–62) regions are underlined. Activities are presented as described in Table I.
The wild-type transcript residues 30–65 is shown underneath with the start of the termination stem–loop shown by underlining.

positions have been changed, but it is apparent, firstly, that the stability of Loop 1 is not related to the efficiency of the AmiR antitermination reaction and, secondly, that some of these residues, particularly **C**CGA**A**C are critical to the process. These sequences thus define the L section of the AmiR recognition site.

Substitutions, insertions and deletions in the sequence from 42–53, the M section, can lead to decreases in the antitermination reaction, and changes towards the 3′ end of the M region have more disruptive effects (Table IIIa). The results with pMW25 and 26, and with pSW62, pSW63, pSW70, pSW71 and pSW73 show that the M region is not critical to antitermination since none of these changes led to complete inactivation. However, the changes at positions 48 and 51 in pMW26 and pSW73 (compared with pSB101 and pSW70 respectively) clearly show that these residues have some importance in the antitermination reaction. Plasmids pSW74 and pSW75 have mutant L regions identical to pSB103 (CgG AtC) which is competent in antitermination, but contain deletions which bring the L and R regions closer together. Both pSW74 and pSW75 show antitermination, although the levels of activity are significantly lower than pSB103 (Table IIIb).

Three plasmids (pMW27, pMW28, pSW72) have been constructed which have changes in the R region (Table IV). All of the (multiple) changes to this region cause severe disruption in the antitermination reaction and show that residues CAC AGA GCA (54–62) are absolutely critical.

To ensure that the leader region mutants were not affected in the level or stability of transcripts produced, and thus that the values obtained in the assays were a direct result of the sequence alterations, transcript levels in the absence of *amiR* were measured by Northern analysis using a labelled *Hin*dII–*Pst*I probe (Table Vb). Apart from pMW26, which shows a somewhat reduced signal compared with pSB101, all of the other mutants analysed showed similar levels of leader transcript, the values of which were independent of the degree of antitermination seen in the presence of AmiR.

Table V. Quantification of leader RNA sequences

	RNA level		
a			
pTM1	44.1		
pTM1,pSW35	103.3		
pSW66	14.8		
b		–AmiR	+AmiR
pSB101	11.0	1.2	42.0
pMW11	8.4	4.6	65.3
pSB103	9.6	1.1	26.0
pSW60	10.6	0	2.4
pMW12	13.2	0.1	3.2
pMW26	5.1	0.3	19.9
pSW74	9.0	2.9	15.4
pMW27	10.4	0.1	1.5

RNA was isolated and quantitated as described in Materials and methods and the results, from which the value of the plasmid free host used was subtracted as background, are presented as arbitrary units.
(**a**) The plasmids were present in strain JM109 (DE3) grown in the absence of IPTG.
(**b**) The plasmids were present in strain JA221 in the absence of *amiR*. The values for amidase activities are abstracted from Tables I–IV.

Analysis of AmiC–AmiR interactions

Previous *in vivo* experiments indicated that AmiC inhibition of AmiR occurred by a protein–protein interaction and suggested there was a stoichiometry between the levels of AmiC and AmiR required to maintain an inducible phenotype (Wilson *et al.*, 1993). These experiments suggested a simple model whereby AmiC inhibited AmiR activity by formation of a complex, sterically hindering the AmiR–RNA interaction.

To test this hypothesis, highly purified AmiC saturated with either acetamide or the anti-inducer butyramide was linked to beads and used as affinity matrices to bind AmiR contained in crude cell-free extracts of *E.coli*, pSW100. The presence of AmiR bound to AmiC could then be detected by Western blot analysis of the proteins bound to the AmiC beads. The results of such an experiment are shown in Figure 3. Beads with BSA attached are unable to bind AmiR (lane 5). Butyramide-saturated AmiC incubated in the presence of excess butyramide forms a complex very inefficiently with AmiR (lane 1). The addition of excess acetamide to butyramide-saturated AmiC (lane 2) allows the efficient formation of an AmiC–AmiR complex. Acetamide would be expected to efficiently displace butyramide from AmiC during complex formation since the K_d for AmiC binding acetamide is ~100-fold lower than that for butyramide (Wilson *et al.*, 1993). Acetamide-saturated AmiC (lane 3) incubated in the presence of excess acetamide efficiently complexes with AmiR. The ability of acetamide-saturated AmiC to bind AmiR in the presence of excess butyramide (lane 4), is reduced. These results show that bead-immobilized AmiC precipitates AmiR in the presence of both inducing and non-inducing amides. One potential problem with the analysis of protein–protein interactions involving solid phase supports is the potential effects of steric hindrance of binding caused by the solid support. This may explain the inabilitiy of butyramide–AmiC to complex efficiently with AmiR, since in free solution they complex efficiently (see below).

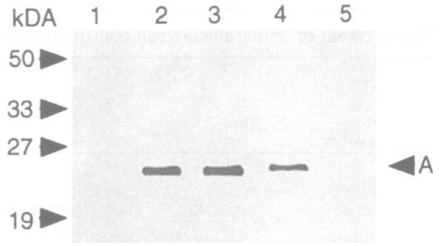

Fig. 3. Analysis of AmiC–AmiR interactions by Western blotting. AmiC–AmiR complexes were prepared and analysed as described in Materials and methods. Lane 1, butyramide-saturated AmiC-beads incubated with AmiR in the presence of 10 mM butyramide; lane 2, butyramide-saturated AmiC-beads incubated with AmiR in the presence of 10 mM acetamide; lane 3, acetamide-saturated AmiC-beads incubated with AmiR in the presence of 10 mM acetamide; lane 4, acetamide-saturated AmiC-beads incubated with AmiR in the presence of 10 mM butyramide; lane 5, BSA-beads incubated with AmiR. The position of AmiR is shown by the ←A on the right.

Isolation and gel filtration analysis of amide–AmiC–AmiR complexes

The data above suggested that in the presence of amides AmiC and AmiR would exist as a complex and could be isolated in this form. Plasmid pRAN1 carrying the *amiC,amiR* genes showed acetamide-inducible, butyramide-repressible amidase activity in *P.aeruginosa*, demonstrating that the regulatory phenotype was maintained with the overexpression of the genes. PAC452, pRAN1 was used for large-scale growth and isolation of the AmiC–AmiR complex in the presence of butyramide as described in Materials and methods. AmiC is 42.8 kDa, AmiR is 21.8 kDa and both migrate as dimers in gel filtration when analysed separately (data not presented). Analytical gel filtration was carried out with pooled AmiC–AmiR fractions from the preparative column in buffer containing butyramide (23 mM), or after addition of acetamide (34 mM) and elution in buffer containing acetamide (Figure 4). The profile of the butyramide run (Figure 4A) shows a single main peak containing equimolar amounts of AmiC and AmiR (C:R ratio 2.0:1, stoichiometry 1:1, RMM = 125 kDa) with a very small AmiC dimer shoulder (RMM = 71 kDa) and a small AmiC monomer peak (RMM = 36 kDa). The acetamide run (Figure 4B) shows a smaller main peak, still containing equimolar amounts of AmiC and AmiR (ratio 2.2:1, stoichiometry 1:1, RMM = 115 kDa) but with shoulders on both sides. The smaller shoulder on the high MW side is AmiR (RMM= 185 kDa) and the large shoulder on the low MW side is AmiC (RMM = 60 kDa). The free AmiR present here probably represents an aggregated form. The addition of acetamide to the AmiC–AmiR complex causes an apparent MW change and partial dissociation of the complex. These results support the most simple explanation for the amide-dependent regulation of amidase activity, that butyramide–AmiC inhibits the antitermination activity of AmiR by complex formation and steric hindrance. However, it is not clear from these data whether free AmiR or an acetamide–AmiC–AmiR complex causes antitermination *in vivo*.

Discussion

The evidence that AmiR is an RNA binding protein comes from titration experiments in which it has been shown

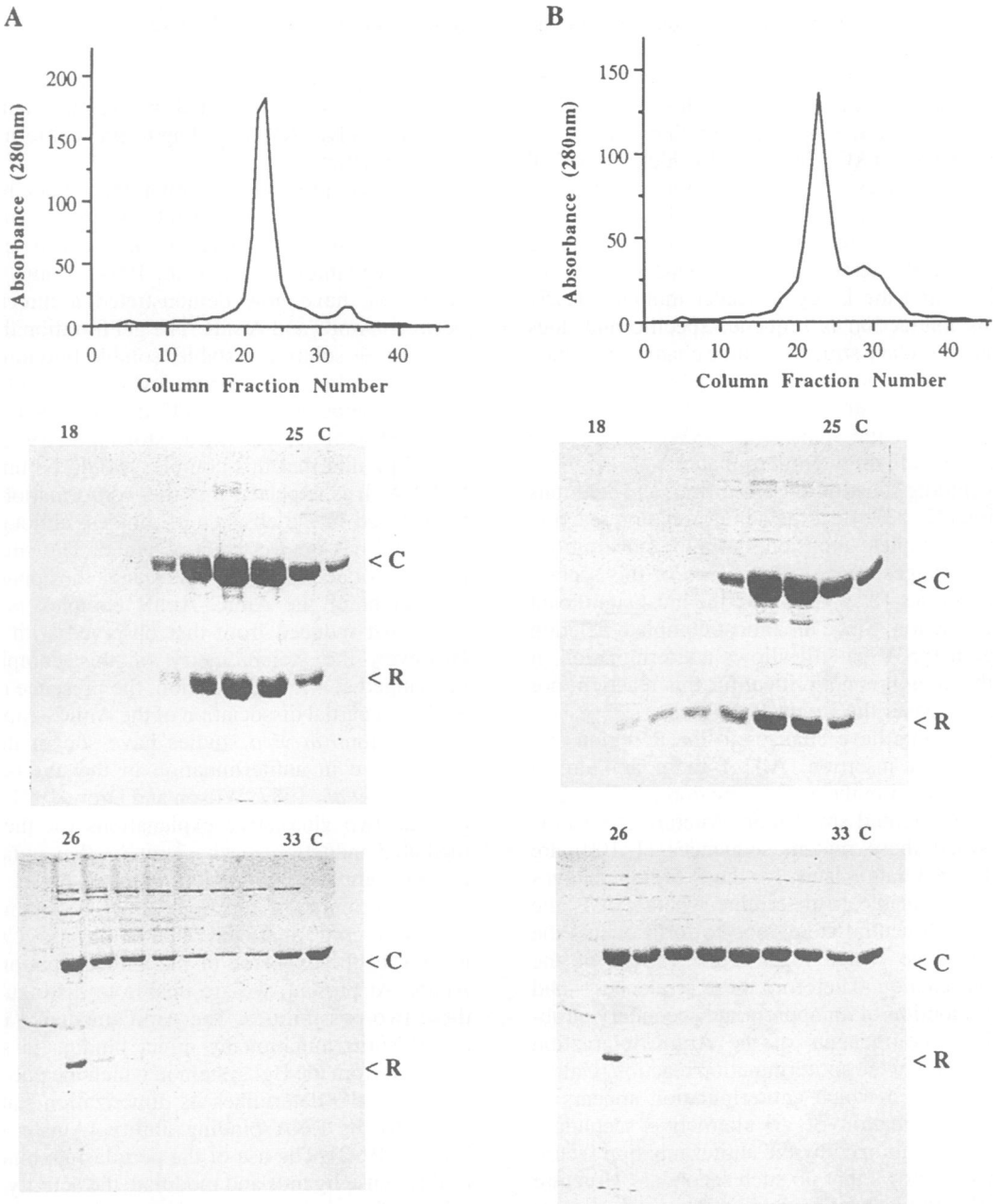

Fig. 4. Superose 12 gel filtration analysis of AmiC–AmiR complexes. (**A**) Elution profile of C/R complex in buffer containing 23 mM butyramide, and SDS–PAGE analysis of fractions. The positions of AmiC and AmiR are shown on the right (<C, <R). (**B**) Elution profile of C/R complex in 23 mM butyramide to which acetamide (34 mM) has been added and the column eluted with acetamide buffer. In both cases fractions 18–25 are present on the upper gel and fractions 26–33 on the lower, and the right-hand lane on each gel contains AmiC as a MW marker.

that production of leader RNA *in trans* partially saturates out the available AmiR, causing a reduction in the AmiR-dependent antitermination activity. The comparison between titration experiments using pSW66 in JA221 and DE3, has clearly established that AmiR interacts with transcripts and not with DNA sequences of the leader region. Additionally, the titration with pSW76 shows that the presence of the first stem–loop is not necessary for AmiR function and that a shortened transcript of residues 35–74 cause titration and thus defines a minimal AmiR binding site. The inability to titrate out AmiR completely in these studies appears to be due to the relatively low expression of competing leader sequences as shown by the Northern analysis.

Studies of the antitermination reaction by mutant analysis showed that the leader ORF had no apparent role in the process and strongly indicated that it was not translated. RNA folding of residues 1–100 of the leader region shows a short, four-residue, 5′ end; a large fairly stable stem–loop 1 (5–37); a central region with the possibility of a small stem–loop at the 3′ end (38–65) and then the large stable termination loop (66–95) (Figure 2). This central region has been broken down further into L (36–41), M (42–53) and R (54–62) sections. Changes to the L region

included substitutions, insertions and deletions, and analysis of the results is made more difficult as some of the changes affect not only the sequence but also the predicted secondary structure and length of stem–loop 1 (unpublished data). From the mutants which show reduced or abolished antitermination it is apparent that changes at two positions CCG AAC (36 and 40) define critical residues. Single changes at either position cause some reduction in antitermination, and double changes almost completely abolish the reaction, presumably reflecting much-reduced AmiR interaction with the leader. Folds (1–100) of pSB101 and the L region leader mutants clearly show that this interaction is sequence-specific and does not depend on secondary structure, since changes in which either the CCG AAC is completely exposed (pMW13), partially incorporated into the stem–loop (pSB102), or completely hidden in the stem–loop (pSW64, 1 residue change from WT), all show antitermination.

Changes including substitutions, insertions and deletions to the M region (42–53) affect the antitermination reaction but none causes complete abolition. From the substitutions it appears that changes towards the 3′ end of this section (CAU ACG: residues 48 and 51) have the most significant effects on the reaction. Since an almost complete deletion of the M region (pSW75) still allows antitermination, it is clear that this region is not critical for this reaction, nor is the spacing between the L and R regions.

Only three mutants have changes to the R region and one (pSW72) is an insertion. All of these are almost completely inactivated in the antitermination reaction, and in each case the potential small loop structure (53–61) is not formed when these mutant sequences (1–100) are folded (unpublished data). Thus, for the R region changes we are at present unable to determine whether it is the failure of the small central stem–loop to form or just the changes in sequence which lead to the failure of the antitermination reaction. Therefore these sequences—and possibly their adoption of an appropriate secondary structure—are critical components of the AmiR interaction with the leader RNA in the antitermination reaction. Unlike the *bgl/sac* systems in which antitermination appears to be mediated by formation of an alternative secondary structure, which is stabilized by the antitermination factor, sequence analysis shows that no such secondary structure is feasible in the amidase leader region. Thus, the tertiary structure of the AmiR RNA binding site is likely to be primarily determined by interactions between the protein and RNA and not by base-pairing within the RNA. There is no sequence similarity between the two critical binding regions L and R and thus the bases are likely to make contact with different regions of the protein, not with the same region on adjacent monomers. Since mutations in either the L or R binding sites abolish antitermination this would suggest that binding to these two sites may be cooperative.

From the mutagenesis studies it is possible that the full extent of the AmiR RNA binding site has not been mapped and could extend further at the 3′ end. Nevertheless, the binding of an AmiR dimer to the RNA in the vicinity of the terminator would be expected to disrupt the formation of the stem–loop structure sufficiently to allow transcription to proceed into *amiE*. Therefore it seems that, mechanistically, AmiR works in a manner analogous to BglG and not lambda N, which involves an interaction and modification of RNA polymerase activity. Consistent with this notion, AmiR appears to work with a variety of different polymerases (*E.coli*, *P.aeruginosa*, T7) suggesting that AmiR-mediated transcription antitermination simply involves RNA binding to prevent terminator stem/loop formation.

We have previously shown that inducing and non-inducing amides bind to AmiC (Wilson *et al.*, 1993) and the crystal structure of AmiC has been determined with bound acetamide (Pearl *et al.*, 1994). Using immobilized AmiC we have now demonstrated a direct interaction between AmiC and AmiR. The gel filtration data indicates that in free solution a stable, soluble butyramide–AmiC–AmiR complex can be isolated whose size and composition are consistent with an AmiC dimer bound to an AmiR dimer (RMM = 125 kDa, stoichiometry 1:1) and we would predict that this complex would be unable to bind to RNA. It is expected that this conformation would also be adopted in the absence of amides, although this form of AmiC has not yet been obtained. The situation in the presence of acetamide is less clear as the apparent molecular weight of the AmiC–AmiR complex is 115 kDa—somewhat reduced from that observed with butryamide. However, the stoichiometry of this complex remains unchanged at ~1:1. In addition, the presence of acetamide leads to a partial dissociation of the AmiC–AmiR complex, and previous *in vivo* studies have shown that AmiR is fully active in antitermination in the absence of AmiC (Cousens *et al.*, 1987; Wilson and Drew, 1991). These data provide two alternative explanations for the acetamide-mediated induction mechanism: (i) that inducer binding causes complex dissociation and free AmiR functions in the antitermination reaction; or (ii) acetamide binding causes a conformational change in the C/R complex leading to the exposure of the antitermination activity of AmiR. At present, we are unable to distinguish between these two possibilities. The AmiC-mediated inhibition of AmiR antitermination by direct binding is substantially different from the Bgl system in which the phosphorylation state of BglG determines its dimerization state, and consequently its RNA binding ability (Amster-Choder and Wright, 1992). The use of the periplasmic binding protein fold to sense ligands and modulate the activity of a nucleic acid binding protein/domain is not unique to AmiC–AmiR. The recently solved structure of the *lac* repressor IPTG binding domain (Friedman *et al.*, 1995) shows it is highly homologous to the arabinose binding protein, and changes in conformation within this domain affect the ability of the DNA binding domain to interact with *lac* operator. However, the *P.aeruginosa* AmiC–AmiR system in which a ligand receptor directly regulates the activity of an RNA binding protein remains unique.

Materials and methods

Construction of plasmids

All plasmid purifications, transformations and clonings were carried out as described previously (Wilson and Drew, 1991). Plasmids pTM1 (pACYC184 derivative; Cm^R; *amiE*) and pSW35 (pKT231 derivative; Sm^R; *amiR* expressed from vector promoter) have been described previously (Wilson and Drew, 1991; Wilson *et al.*, 1993). Plasmid pSW66 was constructed by insertion of the *Fsp*I–*Pst*I (140–450) *amiE* leader fragment from pAS20 (Wilson and Drew, 1991) into *Sma*I–*Pst*I-

cut pGEM3Z (Apr). The leader transcript in pSW66 can only be expressed from the vector T7 promoter. pMW42 was constructed by the insertion of the *Hin*dIII–*Pst*I (1–450) *amiE* leader fragment from pAS20 into *Hin*dIII–*Pst*I-cut pGEM4Z (Apr). With pMW42 the *ami*E leader can be expressed from the vector *lac* and *amiE* promoters and additionally from the vector T7 promoter in an appropriate host. Plasmid pSW76 was made by insertion of the *Bam*I–*Sma*I *amiE* leader fragment (164–203) from pSB102 into *Bam*I–*Hin*II-cut pGEM3Z. The leader transcript from pSW76 can only be expressed from the vector T7 promoter. pSW50 is the maltose binding protein fusion vector pMALC1 (New England Biolabs) carrying the PCR-amplified *amiR* gene. pSW100 is the *tac* promoter-based expression vector pKK223-3 (Pharmacia) carrying the *amiR* gene fragment from pSW50. Plasmid pRAN1 was constructed by PCR amplification of the wild-type *amiC,amiR* genes from strain PAC1 cloned into the broad host range expression vector pMMB66EH (Furste *et al.*, 1986).

Amidase assays

Amidase activity in intact cells was measured as described previously (Wilson *et al.*, 1993). Activity levels presented in this article are the mean values of duplicate assays carried out on at least three separate occasions. One unit represents 1 μmol of acetohydroxamate formed per min. Specific activities presented are units per mg of bacterial cells (Drew, 1984).

DNA manipulations

All plasmid purifications, transformations and cloning were carried out as described previously (Wilson and Drew, 1991).

Site-directed mutagenesis

In vitro mutagenesis was carried out using the Altered Sites™ system (Promega). The *Hin*dIII–*Pst*I (450 bp) and *Hin*dIII–*Xho*I (2391 bp) fragments from pJB950 (Clarke *et al.*, 1981) (Figure 1A) were cloned into pAlter generating respectively, pSB100 and pSB101. pSB100 was used for the oligonucleotide mutagenesis and after mutant characterization the *amiE* gene was 'reconstructed' by insertion of the *Pst*I–*Kpn*I fragment from pJB950. Oligonucleotides were phosphorylated and used as described in the manufacturer's instructions. Mutant plasmids, pSB102, pSB103, pMW10, pMW11, pMW25, pMW26, pMW27 and pMW28 were initially characterized, where possible, by acquisition of new restriction targets and subsequently by DNA sequencing.

Further mutants, derived from the first series, were obtained by *in vitro* manipulation of the parent plasmids pSB102 and 103, pMW25, 26, 27 and 28 which all have unique *Bam*I targets in the leader region. Some derivatives were made by *Bam*I digestion; trimming by S1 nuclease digestion; filling by Klenow fragment and dNTPs and ligation by T4 DNA ligase. Other plasmids were made after *Bam*I cleavage, by joining the left (L) arm of one plasmid with the right (R) arm of a second. This was carried out by ligation of the gel-purified small *Eco*RI–*Bam*I fragment from one parent with the large *Eco*RI–*Bam*I fragment from the other parent. After transformation recombinants were characterized by restriction mapping.

DNA sequencing

Confirmation of sequences after *in vitro* mutagenesis and subsequent manipulations was carried by sequencing double-stranded plasmid DNA as described previously (Wilson and Drew, 1991).

RNA analysis

Total RNA was prepared from *E.coli* grown to late log phase using the Ultraspec RNA Isolation System (Biotecx Laboratories, Inc.) according to the manufacturer's instructions. RNA was quantified spectrophotometrically and 5 μg of each RNA sample applied to a slot–blot apparatus as described in Sambrook *et al.* (1989). The *Hin*dIII–*Pst*I leader fragment from pAS20 was used as a probe by random oligonucleotide labelling using a DNA labelling kit (Pharmacia) and [α-^{32}P]CTP according to the manufacturer's instructions. The slot–blot was probed using the conditions described previously (Wilson and Drew, 1995) and the amount of *amiE* leader RNA quantitated using a Phosphorimager (Molecular Dynamics) after overnight counting.

Western blotting

Semi-dry Western blotting onto nitrocellulose filters was carried out using the Novablot system (Pharmacia), according to the manufacturer's instructions. Western blots were incubated overnight with the AmiR antibody at a dilution of 1:1000 in 1× TBS (25 mM Tris–HCl, pH 7.2, 150 mM NaCl) in the presence of 1% dried milk. Subsequently, the blots were washed three times in 1× TBS and then incubated for 1 h in 1× TBS + 1% dried milk with a 1:1000 horseradish peroxidase anti-rabbit conjugate secondary antibody (Sigma) for 1 h. Western blots were subsequently washed twice in 1× TBS and developed using 4-chloro-1-napthol.

Purification of AmiC, AmiR and AmiC–AmiR complexes

AmiC was purified as described previously (Wilson *et al.*, 1991). Butyramide- and acetamide- saturated AmiC were prepared by extensive dialysis against buffer A (20 mM Tris–HCl, pH 8.0, 1 mM DTT, 1 mM EDTA) supplemented with the respective amides at a concentration of 10 mM.

The maltose-binding protein–AmiR fusion protein was prepared using amylose affinity chromatography according to the manufacturer's instructions (New England Biolabs). The MBP–AmiR protein for immunization was dialysed against 1× PBS (100 mM NaCl, 20 mM Tris–HCl, pH 7.4, 1 mM EDTA) prior to raising a rabbit antiserum.

The AmiC–AmiR complex was isolated as follows: PAC452pRAN1 was grown at 37°C in Nutrient broth 2 (Oxoid) plus 23 mM butryamide to mid-exponential growth phase and *amiC, amiR* expression was induced by addition of 3 mM IPTG. Growth was continued for 14 h and the cells harvested by centrifugation at 5000 *g* at 4°C, in a Sorvall RC2B for 30 min. Cell pellets were resuspended in buffer B (50 mM Tris, pH 8.0, 1 mM DTT, 1 mM EDTA, 1 mM PMSF, 23 mM butyramide) and sonicated as described previously (Wilson and Drew, 1991). Cell-free extracts were prepared by centrifugation (15 000 *g*, 4°C, 30 min). The cleared lysate was ammonium sulfate-precipitated and the 40–50% fraction was resuspended in buffer B. The ammonium sulfate cut was fractionated by FPLC (Pharmacia) gel filtration. 1 ml of extract was loaded onto a preparative column (Superdex 200, HiLoad 16/60) and eluted with buffer B + 150 mM NaCl. 1 ml fractions were collected and 150 μl aliquots were TCA-precipitated and the proteins resolved by SDS–PAGE for identification of the AmiC–AmiR complex. AmiC was detected by co-migration with purified AmiC and AmiR by Western blotting. Fractions containing the largest amounts of the complex were pooled for analytical gel filtration.

AmiC–AmiR complex assays

For bead assays, purified AmiC and BSA were covalently linked to Affigel 15 (Bio-Rad) according to the manufacturer's instructions. AmiC–Affigel beads (50 ml) were incubated with crude extracts containing AmiR in buffer C (20 mM Tris–HCl, pH 8.0, 1 mM DTT, 1 mM EDTA, 150 mM NaCl) for 1 h at room temperature with gentle agitation. Beads were then centrifuged briefly at 12 000 *g*, given three, 20 min washes in 2 ml of buffer C, and finally resuspended in SDS–PAGE sample buffer. Samples were boiled to dissociate complexes and the resulting supernatant subjected to Western blot analysis using the AmiR antibody as described above.

For gel filtration assays, pooled preparative fractions were analysed using a Superose12 gel filtration column (Pharmacia). Samples were initially in buffer B (containing 23 mM butyramide). Acetamide (34 mM) was added, where necessary, and samples incubated at 25°C for 60 min. 0.2 ml fractions were collected after elution with buffer containing either 23 mM butyramide or 34 mM acetamide and TCA-precipitated. The precipitate was dissolved, proteins resolved by SDS–PAGE and the amount of material present determined by analysis with an Imaging Densitometer (Bio-Rad) using Molecular Analyst/Macintosh Software. The Superose 12 column was calibrated using gel filtration standards (Pharmacia).

Acknowledgements

Many thanks are due to Sharon Banin, who constructed some of the leader sequence mutations. S.A.W. was supported by a Wellcome Trust grant to R.E.D. and L.H.P., S.J.M.W. was supported by a British Council (TDA) Studentship and R.A.N. is a BBSRC research student.

References

Amster-Choder,O. and Wright,A. (1992) Modulation of the dimerization of a transcriptional antiterminator protein by phosphorylation. *Science*, **257**, 1395–1398.

Amster-Choder,O. and Wright,A. (1993) Transcriptional regulation of the *bgl* operon of *Escherichia coli* involves phosphotransferase system-mediated phosphorylation of a transcriptional antiterminator. *J. Cell. Biochem.*, **51**, 83–90.

Aymerich,S. and Steinmetz,M. (1992) Specificity determinants and structural features in the RNA target of the bacterial antiterminator proteins of the BglG/SacY family. *Proc. Natl Acad. Sci. USA*, **89**, 10410–10414.

Brammar,W.J. and Clarke,P.H. (1964) Induction and repression of *Pseudomonas aeruginosa* amidase. *J. Gen. Microbiol.*, **37**, 307–319.

Clarke,P.H., Drew,R.E., Turberville,C., Brammar,W.J., Ambler,R.P. and Auffret,A.D. (1981) Alignment of the cloned *amiE* gene of *Pseudomonas aeruginosa* with the N-terminal sequence of amidase. *Biosci. Rep.*, **1**, 299–307.

Cousens,D.J., Clarke,P.H. and Drew,R.E. (1987) The amidase regulatory gene (*amiR*) of *Pseudomonas aeruginosa*. *J. Gen. Microbiol.*, **133**, 2041–2052.

Drew,R.E. (1984) Complementation analysis of the aliphatic amidase genes of *Pseudomonas aeruginosa*. *J. Gen. Microbiol.*, **130**, 3101–3111.

Drew,R.E. and Lowe,N. (1989) Positive control of *Pseudomonas aeruginosa* amidase synthesis is mediated by a transcription antitermination mechanism. *J. Gen. Microbiol.*, **135**, 817–823.

Friedman,A.M., Fischmann,T.O. and Steitz,T.A. (1995) Crystal structure of *lac* repressor core tetramer and its implications for DNA looping. *Science*, **268**, 1721–1727.

Furste,J.P., Pansegrau,W., Frank,R., Blocker,H., Scholz,P., Bagdasarian,M. and Lanka,E. (1986) Molecular cloning of the plasmid RP4 primase region in a multi-host-range *tacP* expression vector. *Gene*, **48**, 119–131.

Jaeger,J.A., Turner,D.H. and Zuker,M. (1989a) Improved predictions of secondary structures for RNA. *Proc. Natl Acad. Sci. USA*, **86**, 7706–7710.

Jaeger,J.A., Turner,D.H. and Zuker,M. (1989b) Predicting optimal and suboptimal secondary structure for RNA. In Doolittle,R.F. (ed.), *Molecular Evolution: Computer Analysis of Protein and Nucleic Acid Sequences. Methods Enzymol.*, **183**, 281–306.

Kelly,M. and Clarke,P.H. (1962) An inducible amidase produced by a strain of *Pseudomonas aeruginosa*. *J. Gen. Microbiol.*, **27**, 305–316.

Le Coq,D., Crutz,A.M., Richter,R., Aymerich,S., Gonzy-Treboul,G., Zagorec,M., Rain-Guion,M.C. and Steinmetz,M. (1989) Induction of levansucrase by sucrose in *Bacillus subtilis*: involvement of an antitermination mechanism negatively controlled by the PTS. In Butler,L.O., Harwood,C. and Moseley,B.E.B. (eds), *Genetic Transformation and Expression*. Intercept Ltd., Andover, UK, pp. 447–456.

Lowe,N., Rice,P.M. and Drew,R.E. (1989) Nucleotide sequence of the aliphatic amidase regulator gene (*amiR*) of *Pseudomonas aeruginosa*. *FEBS Lett.*, **246**, 39–43.

Mahadevan,S. and Wright,A. (1987) A bacterial gene involved in transcription antitermination: regulation at a rho-independent terminator in the *bgl* operon of *E. coli*. *Cell*, **50**, 485–494.

Pearl,L., O'Hara,B., Drew,R. and Wilson,S. (1994) Crystal structure of AmiC: the controller of transcription antitermination in the amidase operon of *Pseudomonas aeruginosa*. *EMBO J.*, **13**, 5810–5817.

Roberts,J.W. (1988) Phage lambda and the regulation of transcription termination. *Cell*, **52**, 5–6.

Sambrook,J., Fritsch,E.F. and Maniatis,T. (1989) *Molecular Cloning: A Laboratory Manual*, 2nd edn. Cold Spring Harbor Laboratory Press, Cold Spring Harbor, NY.

Squires,C.L., Greenblatt,J., Li,J., Condon,C. and Squires,C.L. (1993) Ribosomal RNA antitermination *in vitro*: requirement for Nus factors and one or more unidentified cellular components. *Proc. Natl Acad. Sci. USA*, **90**, 970–974.

Wilson,S.A. and Drew,R.E. (1991) Cloning and DNA sequence of *amiC*, a new gene regulating expression of the *Pseudomonas aeruginosa* aliphatic amidase, and purification of the *amiC* product. *J. Bacteriol.*, **173**, 4914–4921.

Wilson,S.A. and Drew,R.E. (1995) Transcriptional analysis of the amidase operon from *Pseudomonas aeruginosa*. *J. Bacteriol.*, **177**, 3052–3057.

Wilson,S.A., Chayen,N.E., Hemmings,A.M., Drew,R.E. and Pearl,L.H. (1991) Crystallisation of and preliminary X-ray data for the negative regulator (AmiC) of the amidase operon of *Pseudomonas aeruginosa*. *J. Mol. Biol.*, **222**, 869–871.

Wilson,S.A., Wachira,S.J., Drew,R.E., Jones,D. and Pearl,L.H. (1993) Antitermination of amidase expression in *Pseudomonas aeruginosa* is controlled by a novel cytoplasmic amide-binding protein. *EMBO J.*, **12**, 3637–3642.

Zuker,M. (1989) On finding all suboptimal foldings of an RNA molecule. *Science*, **244**, 48–52.

Received on January 11, 1996; revised on May 31, 1996